ELSEVIER

Ultrasonics 40 (2002) 269–274

Ultrasonics

www.elsevier.com/locate/ultras

Multiple scattering of seismic waves

N. Trégourès [a], R. Hennino [b], C. Lacombe [b], N.M. Shapiro [c], L. Margerin [b], M. Campillo [b], B.A. van Tiggelen [a,*]

[a] *Laboratoire de Physique et Modélisation des Milieux Condensés, CNRS/Université Joseph Fourier, Maison des Magistères, B.P. 166, 38042 Grenoble, France*

[b] *Laboratoire de Géophysique Interne et Tectonophysique, Observatoire de Grenoble, Université Joseph Fourier/CNRS, B.P. 53, 38041 Grenoble Cedex 09, France*

[c] *Department of Physics, University of Colorado at Boulder, Campus Box 390, Boulder, CO 80309-0390, USA*

Abstract

We present theory and numerical simulations to model seismic wave propagation in the Earth crust. We compare them to observations made in Mexico. © 2002 Elsevier Science B.V. All rights reserved.

Keywords: Seismology; Multiple scattering

1. Introduction

The seismic coda refers to the pronounced exponential time tail observed in the seismograms of regional earthquakes in the frequency band 1–10 Hz, reaching the level of seismic noise after sometimes more than 10 times the travel time of direct waves. Many recent studies have made an attempt to relate physical properties of the Earth lithosphere to the observed regional seismic coda. This relation is suggested by the observational fact that the time decay coefficient of the energy in the seismic coda, the coda Q factor, is seen to be a regional constant [1,2], dependent on frequency, but largely independent on details of the seismic source, such as distance, depth, magnitude and orientation. Whereas early work [1,3,4] tried to model the coda as singly scattered waves in a uniform space, recent numerical studies suggested the importance of multiple scattering [5–8]. Coda signals often extend to more than 200 s, and their possible interpretation as a genuine multiple scattering phenomenon is in order. The recognition of multiple scattering would facilitate the application of many "mesoscopic tools", developed in the last decennium in condensed matter physics, optics and acoustics [9] in the understanding and modeling of seismic data, with the ultimate goal to do the inverse problem.

Several phenomena studied in ultrasonics, such as equipartition [10], coherent backscattering [11] and "ultrasonics without a source" [12], are now under active study in seismology.

2. Modelisation of seismic multiple scattering

Our first challenge is to come to a quantitative model for the characteristic decay of the seismic coda, and to see if multiple scattering can explain the observed decays. Empirically, the elastic (kinetic) energy measured after an earthquake is described by the formula [1]

$$\rho(t) \sim \frac{1}{t^n} \exp\left(\frac{-2\pi f t}{Q_c}\right), \tag{1}$$

where n is a number between 1 and 2, f is the frequency, and Q_c an empirical parameter that quantifies the coda. The latter is known to be largely independent of location, distance and magnitude of the earthquake and is therefore believed to be a local characteristic of the Earth crust. It depends on frequency and also varies a lot across the Earth [13,14], typically between 50 and 1000.

The physical interpretation of Q_c and its relation to scattering and intrinsic absorption of the lithosphere are

* Corresponding author. Fax: +33-4-76-88-79-81.

E-mail address: bart.van-tiggelen@labs.polycnrs-gre.fr (B.A. van Tiggelen).

PII: S0041-624X(02)00105-1

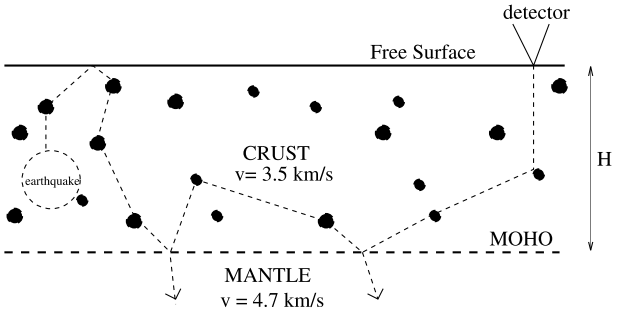

Fig. 1. Geometry for which the radiative transfer equation is solved.

still actively debated [5,15,16]. We have developed a Monte-Carlo program that calculates the scattering of acoustic waves from small random impurities, treated in the Born approximation [17]. We confined the scatterers in a geometry that is known to be relevant for seismic wave propagation in the frequency band 1–20 Hz (Fig. 1): A heterogeneous crust having a depth of roughly 30 km, overlying a rather homogeneous mantle, covered by a free surface. The wave speeds are higher in the mantle than in the crust (by a factor of roughly 1.4), implying the possibility of guided waves [18].

For an "optically thick" crust, i.e. when its mean free path is smaller than its depth $H \approx 30$ km, multiple scattering can be modeled by a diffusion equation [17],

$$\partial_t \rho(\mathbf{r},t) - D\nabla^2 \rho(\mathbf{r},t) + \frac{1}{\tau_a}\rho(\mathbf{r},t) = K\delta(\mathbf{r}-\mathbf{r}_0)\delta(t), \qquad (2)$$

where τ_a is the absorption time and $D = \frac{1}{3}v\ell^*$ is the diffusion constant in terms of the (dominating S) wave velocity, and the transport mean free path ℓ^*. At large lapse time the solution of the diffusion equation, supplied by the boundary conditions is simply,

$$\rho(\mathbf{r},t) \sim \frac{1}{Dt}\exp\left(-\frac{r^2}{4Dt}\right)\exp\left(-\frac{Dt\xi_0^2}{H^2} - \frac{t}{\tau_a}\right), \qquad (3)$$

with ξ_0 the smallest root of the eigenvalue equation $\xi \tan \xi = H/z_0\ell^*$, where $z_0 \approx 1$ for the Moho.

The resemblance of this solution to the empirical relation (1) is striking. It is consistent with $n = 1$ and suggests the following expression for the Coda Q,

$$\frac{1}{Q_c(f)} = \frac{D\xi_0^2}{2\pi f H^2} + \frac{1}{Q_i}. \qquad (4)$$

The first term on the right hand side represents the "leakage" of energy into the mantle, hindered by internal reflection and multiple scattering. The second term stands for the intrinsic inelastic effects, with $Q_i \equiv 2\pi f \tau_a$. Since the absorption of elastic energy per cycle $T = 1/f$ is likely to be a constant, Q_i depends only weakly on frequency. Eq. (4) suggests that inelastic effects dominate the physics of Coda Q at high frequencies. At smaller frequencies, scattering dominates, and observations suggest that $Q_c \sim f$. This would imply a *frequency-independent* diffusion constant, consistent with small fluctuations with a correlation length large compared to the wavelength (the so-called Rayleigh–Gans regime). An amusing, so far non-observed feature of Eq. (2) is that the diffuse maximum propagates along the surface with the subsonic velocity $v_D = \frac{2}{3}v\ell^*/H$.

The above analysis, and hence Eq. (4), hold only in the diffuse regime $\ell^* < H$. Nevertheless, our simulations

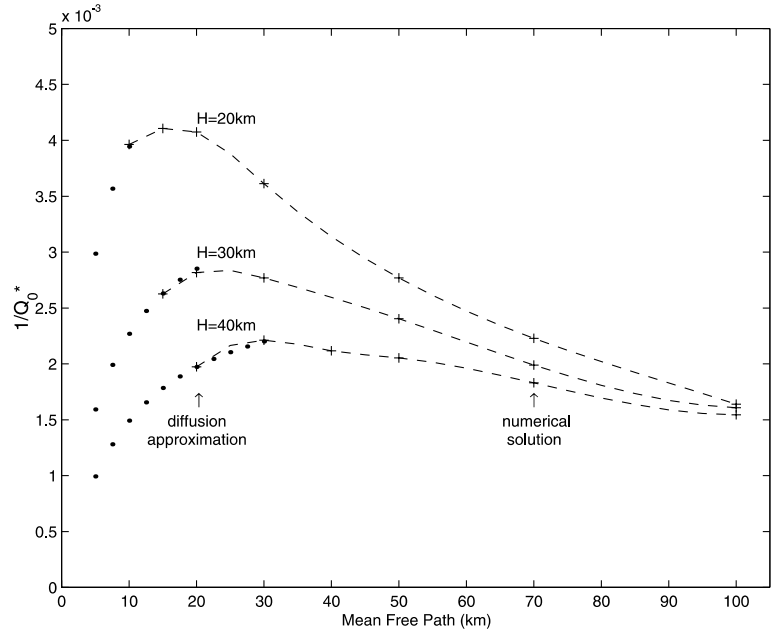

Fig. 2. Numerical solution for the inverse coda quality factor $1/Q_c$ at 1 Hz of acoustic waves in a crust of depth H, as a function of its mean free path ℓ^*. A velocity contrast $v_M/v_C = 1.35$ between mantle and crust has been adopted.

have confirmed their validity for all values for ℓ^*/H, though with the first term modified. Fig. 2 shows the numerical solution for Q_c of the full (acoustic) radiative transfer equation without absorption. For small mean free paths, the diffusion approximation applies and $1/Q_c$ *increases* with increasing mean free path, i.e. with decreasing heterogeneity. For large mean free paths the opposite occurs: $1/Q_c$ *decreases* with mean free path. In this regime, the coda is caused by leakage of energy limited by the rate with which guided modes are singly scattered into "leaky" modes who, for a velocity mismatch 1.32 at the Moho, disappear on a rapid time scale H/v. Hence in this regime,

$$\frac{1}{Q_c} \approx \frac{1}{2\pi f \tau_G} + \frac{1}{Q_i}, \tag{5}$$

with $\tau_G \approx v\ell$ the extinction time of guided waves.

3. Observations of coda in Mexico

We have considered a data set of 45 local earthquakes [19], with a maximum epicentral distance less than 50 km, recorded at stations CAIG, HUIG, PNIG and ZIIG of the Mexican broad-band network [20], located along the Mexican coast. All events showed a clear exponential coda decay, obeying the law (1).

Fig. 3 shows the observed parameter $1/Q_c$ as a function of frequency, showing it to decay roughly as $1/f$ at small frequencies, before it saturises at larger frequencies. This can be explained by the relation (4), if one assumes, quite reasonably, that Q_i is independent of f, and that the mean free path varies slowly in this regime (dashed lines). For $Q_i = 1000$, $H = 30$ km, and the observed value $Q_c = 240$ at $f = 1$ Hz, Eq. (4) provides $\ell^* \approx 20$ km, which would put the Mexican crust well in the multiple scattering regime. Note that Fig. 2 *excludes* a Moho depth $H > 30$ km.

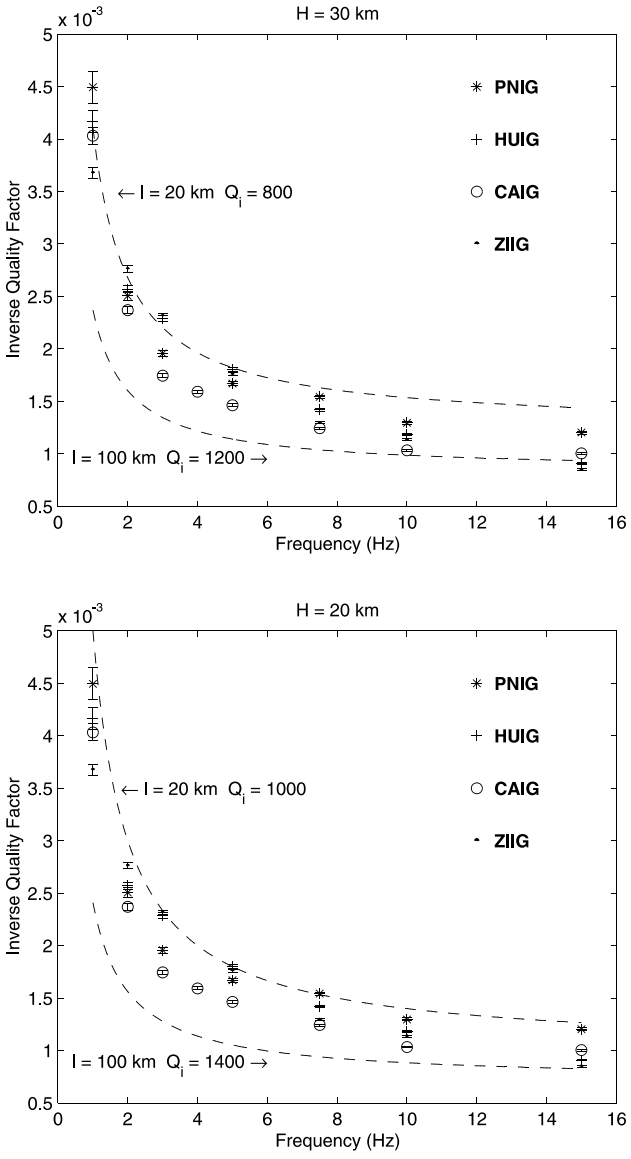

Fig. 3. Observed values for Q_c at different stations, as a function of frequency. Dashed lines show the predictions of multiple scattering theory, for two different depths of the Moho, assuming a constant absorption $Q_i = 1000$, and different mean free paths.

4. Equipartition of seismic waves

One of our main challenges was to find a model-independent confirmation of the pertinence of multiple scattering. To this end, we have investigated the principle of *equipartition* [10,21–23], based on the fact that multiple scattering tends to homogenize phase space: the spectral energy density at a specified frequency, originally distributed in phase space in a fashion that largely depends on the nature of the source, eventually becomes uniform. Although a genuine consequence of multiple scattering, equipartition has the remarkable property to be independent of the unknown fluctuations that cause the scattering.

If $\mathbf{u}(\mathbf{r},t)$ is the local, time-dependent displacement vector in some small frequency band, it can be expanded into the eigenfunctions $\mathbf{u}_n$ of the elastic medium with eigenfrequency ω_n,

$$\mathbf{u}(\mathbf{r},t) = \sum_n \varepsilon_n e^{-i\omega_n t}\mathbf{u}_n(\mathbf{r}) \tag{6}$$

In the presence of disorder, all modes get mixed and the ε_n become time-dependent random variables. The simplest way of expressing equipartition is that the average $\langle\varepsilon_n\rangle = 0$ and that $\langle\varepsilon_n\varepsilon_m^*\rangle = \sigma^2(t)\delta_{nm}$ [24]. It can easily be verified that this statement implies an "equipartition" of elastic energy (7) among the different modes.

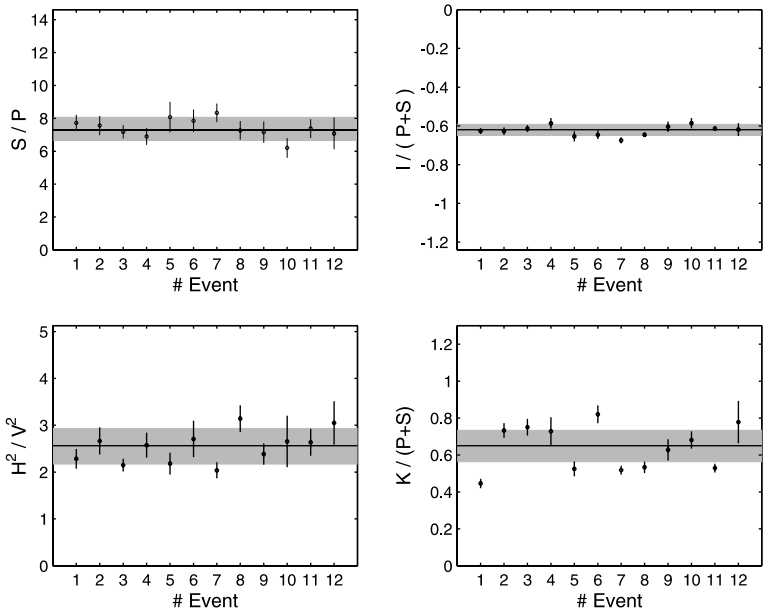

Fig. 4. Observed time-averaged energy ratios S/P of shear to compressional energy (top right), $K/(S+P)$ of kinetic to potential energy (top left), H^2/V^2 of horizontal displacements to vertical displacement (bottom right) and $I/(P+S)$ surface interference to potential energy. The solid line denotes the mean value adopted for the ensemble-average. The error bars estimate the standard deviation from their average, which is much larger than the time-dependent fluctuations around the average for one event.

The total elastic wave energy density is given by [25]

$$W(\mathbf{r},t)=\frac{1}{2}\rho(\partial_t\mathbf{u})^2+\frac{1}{2}(\lambda+2\mu)(\mathrm{div}\,\mathbf{u})^2+\frac{1}{2}\mu(\mathrm{curl}\,\mathbf{u})^2+I. \tag{7}$$

Here ρ denotes the mass density. In our study, the Lamé coefficients λ and μ of the strain–stress tensor are assumed constant and equal in the Earth's crust. The different terms represent, respectively, kinetic (K), compressional (P), and shear (S) energy density. The last term (I) is an interference term involving cross-terms of the kind $\partial_i u_j \partial_k u_l$ that only persists near boundaries. We also investigated the ratio of kinetic energies u_i^2 for elastic displacements in different directions.

The derivatives "div" and "curl" discriminate between transverse and longitudinal displacements. The aperture array used by us, a 50 m side square [26], was temporarily set up close to the city of Chilpancingo (Mexico). The high seismic rate in Mexico made it possible to record, during the three months of the experiment, a series of local earthquakes with magnitudes between 4 and 5, and a spread of roughly 300 km in epicentral distance. The three vertical derivatives $\partial_z u_i$ were deduced from the measured two horizontal partial derivatives by imposing the stress free condition at the local Earth surface.

In the regime of seismic coda, all energy ratios saturise until the signal-to-noise level is reached [27]. The first arrivals were also investigated but their energy ratios were seen to exhibit very large fluctuations. Fig. 4 show that the measured energy ratios are roughly the same for all 12 sources, in spite of their large variations

Table 1
Observed averaged energy ratios (in the frequency range 1–3 Hz, with standard deviation) compared to theory [27][a]

Energy ratio	Data	Exact theory			Theory ($z=0$)	
	$z=0$	$z=0$	$z=\frac{1}{2}\lambda$	$z=\infty$	Rayleigh only	Bulk only
S/P	7.47 ± 0.57	7.19	6.76	10.39	6.460	9.76
$K/(S+P)$	0.59 ± 0.12	0.534	1.03	1	0.268	1.19
$I/(S+P)$	-0.63 ± 0.02	−0.617	0.334	0	−1.464	−0.336
H^2/V^2	2.38 ± 0.34	1.774	2.96	2	0.464	4.49
X^2/Y^2	0.6 ± 0.20	1	1	1	1	1

[a] The kinetic, compressional, shear and interference contributions to the elastic energy in Eq. (7) are denoted by K, P, S and I; $H^2=X^2+Y^2$ denotes the kinetic energy involved in the horizontal motion, V^2 the one in the vertical motion. The third column is calculated by considering bulk and Rayleigh waves. It also shows the predicted depth dependence of the ratios. The forth column is calculated by considering the surface Rayleigh waves only while the last column is calculated by considering bulk waves only.

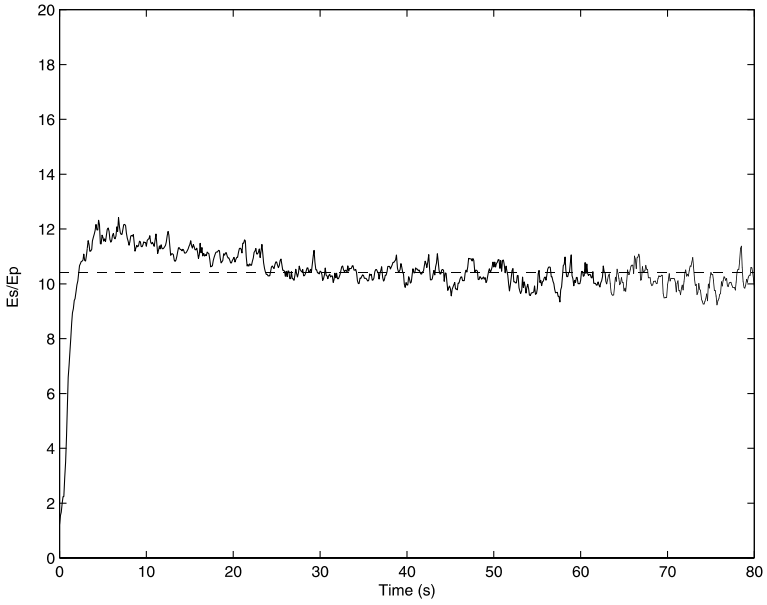

Fig. 5. Simulated equipartition process for elastic waves scattered by Rayleigh scatterers, with a mean free path $\ell = 10$ km (mean free time 3 s). Detection occurs close to the source, which has been assumed here to be purely compressional (i.e. an explosion). The dashed line denotes the theoretical value 10.36 for the infinite medium.

in seismic magnitude and distance. Especially the variation of $I/(S+P)$ is weak, only 3%. Its non-zero value indicates the role of mode conversions at the Earth's surface.

We interpret the observed time-independent energy ratios as a sign of equipartition, and will calculate them for a random Poissonian ($\lambda = \mu$) medium, bounded by a free surface. The values for the infinite medium, $\langle I \rangle = 0$, $\langle K \rangle / \langle S+P \rangle = 1$ and $\langle S \rangle / \langle P \rangle = 10.39$ [10,22], are in clear disagreement with the observations. A more realistic model should take into account the mode conversions at the Earth's free surface. In that case all equipartition ratios oscillate near the free surface and finally converge towards the bulk values (Table 1). Apart from the two kinetic ratios (that we will not discuss here), the values at the surface agree very well with observations. In particular, Table 1 shows that the Rayleigh surface waves should participate in the equipartition process to come to a quantitative agreement.

What useful information can be retrieved from the equipartition process? The theoretical expectation is that it takes typically one mean free time for the modes to equipartition. As a result, the equipartioning process should be immediate for receivers at distances $r > \ell^*$ from the source. Fig. 5 shows the equipartition process obtained from a Monte-Carlo simulation of elastic waves in a layer geometry, and for an explosion source. Very near the source, as in Fig. 5, equipartition sets in after roughly one mean free time (here 35 s).

This work was supported by the program *Intérieur de la Terre* of the INSU/CNRS, the *Groupement de Recherches 1847 PRIMA* of the CNRS, and the Mexican CONACYT project J32308-T. We are also indebted to S.K. Singh, and R. Weaver for their help and support.

References

[1] K. Aki, J. Geoph. Res. 74 (1969) 615.
[2] K. Aki, B. Chouet, J. Geoph. Res. 80 (1975) 3322.
[3] H. Sato, J. Phys. Earth 25 (1977) 27.
[4] M. Herraiz, A.F. Spinoza, Pure Appl. Geoph. 125 (1997) 1569.
[5] I.R. Abubakirov, A.A. Gusev, Phys. Earth Plan. Int. 64 (1990) 52.
[6] M. Hoshiba, Phys. Earth. Plan. Int. 67 (1991) 123.
[7] H. Sato, Geoph. J. Int. 112 (1993) 141.
[8] R.S. Wu, K. Aki, Pure Appl. Geoph. 128 (1988) 49.
[9] New Aspects of Electromagnetic and Acoustic Wave Diffusion, Springer-Verlag, Heidelberg, 1998, edited by POAN Research Group.
[10] R.L. Weaver, J. Acoust. Soc. Am. 71 (1982) 1608.
[11] J. de Rosny, A. Tourin, M. Fink, Phys. Rev. Lett. 84 (2000) 1693–1696;
A. Tourin, A. Derode, Ph. Roux, B.A. van Tiggelen, M. Fink, Phys. Rev. Lett. 79 (1997) 3637–3641.
[12] R.L. Weaver, O.I. Lobkis, Phys. Rev. Lett. 134301 (2001) 1–4.
[13] S.K. Singh, R.B. Hermann, J. Geoph. Res. 88 (1983) 527.
[14] A. Jin, K. Aki, Bull. Seism. Soc. Am. 78 (1988) 741.
[15] M. Hoshiba, J. Geoph. Res. 98 (1993) 15809;
Geoph. Res. Lett. 21 (1994) 2853.
[16] A. Gusev, Geoph. J. Int. 123 (1995) 665.
[17] L. Margerin, M. Campillo, B.A. van Tiggelen, Geoph. J. Int. 134 (1998) 596.
[18] K. Aki, P.G. Richards, Quantitative Seismology: Theory and Methods, Freeman, San Francisco, 1980;
T. Lay, T.C. Wallace, Modern Global Seismology, Academic Press, San Diego, 1995.
[19] L. Margerin, M. Campillo, N.M. Shapiro, B.A. van Tiggelen, Geoph. J. Int. 138 (1999) 343.

[20] S.K. Singh, J. Pacheco, F. Courboulex, D.A. Novelo, J. Seism. 1 (1997) 39.
[21] R.L. Weaver, J. Mech. Phys. Solids 38 (1990) 55–86.
[22] G.C. Papanicolaou, L.V. Ryzhik, J.B. Keller, Bull. Seism. Soc. Am. 86 (1996) 1107.
[23] J.A. Turner, Bull. Seism. Soc. Am. 88 (1998) 276.
[24] R.L. Weaver, J. Acoust. Soc. Am. 78 (1985) 131.
[25] P.M. Morse, H. Feshbach, Methods of Theoretical Physics, McGraw-Hill, NY, 1953.
[26] N. Shapiro, M. Campillo, L. Margerin, S.K. Singh, V. Kostoglodov, J. Pacheco, Bull. Seism. Soc. Am. 90 (2000) 655.
[27] R. Hennino, N. Trégourès, N.M. Shapiro, L. Margerin, M. Campillo, B.A. van Tiggelen, R.L. Weaver, Phys. Rev. Lett. 86 (2001) 3447.